

**THE THICKNESS OF MERCURY'S LITHOSPHERE INFERRED FROM MESSENGER GRAVITY AND TOPOGRAPHY.**

Peter B. James<sup>1</sup>, Roger J. Phillips<sup>2</sup>, Matthias Grott<sup>3</sup>, Steven A. Hauck, II<sup>4</sup>, and Sean C. Solomon<sup>1,5</sup>, <sup>1</sup>Lamont-Doherty Earth Observatory, Columbia University, Palisades, NY 10964, USA (peterj@ldeo.columbia.edu), <sup>2</sup>Planetary Science Directorate, Southwest Research Institute, Boulder, CO 80302, USA, <sup>3</sup>Institute of Planetary Research, German Aerospace Center (DLR), Rutherfordstraße 2, 12489 Berlin, Germany, <sup>4</sup>Department of Earth, Environmental, and Planetary Sciences, Case Western Reserve University, Cleveland, OH 44106, USA, <sup>5</sup>Department of Terrestrial Magnetism, Carnegie Institution of Washington, Washington, DC 20015, USA.

**Elastic deformation:** The thickness of a planetary lithosphere is often expressed in terms of an effective elastic thickness  $T_e$ , which represents the thickness of an idealized plate that reproduces the observed flexural signatures. This quantity can be interpreted in terms of the thickness  $T_m$  of a mechanical lithosphere, which is the portion of the planet's rigid outer shell that can maintain stresses over geological time [1]. A lithosphere will flex in response to an applied load (e.g., cratering, extrusive and intrusive igneous deposits), and the amount of flexure depends on the wavelength of the load [2,3]. This wavelength-dependent flexural response produces characteristic admittance functions (the spectral ratio of gravity over topography) and correlation functions (the spectral correlation of gravity and topography) [4].

**MESSENGER observations:** Recent improvements from MESSENGER in the gravity field [5] and topography [6] for Mercury open the door for a more robust analysis of lithosphere thickness via spectral comparisons of gravity and topography. We calculated admittance and correlation spectra in Mercury's northern hemisphere using a zonal Slepian taper with a bandwidth of degree  $L=2$  and a localization radius of  $90^\circ$ . Global correlation is less than the localized northern hemisphere correlation at most wavelengths, but this result may reflect the difference in data quality between the northern and southern hemispheres rather than a geological difference. The observed admittance and correlation of topography reflect the state of the lithosphere at the time of topographic formation (the first  $\sim 1$  Gyr of Mercury's history).

**The influence of data noise:** Most simple compensation mechanisms (including crustal compensation) are associated with unitary correlation of gravity  $g$  and topography  $h$ . Non-unitary correlations of gravity and topography indicate the existence of multiple compensation mechanisms, noise in the gravity dataset, or both. The observed gravity signal  $g_{obs}$  is a combination of the true gravity signal  $g_{true}$  and data noise  $I$ :

$$g_{obs} = g_{true} + I \quad (1)$$

These terms may be interpreted as spatial or spectral quantities. Insofar as  $I$  is uncorrelated with topography, the estimation of admittance is not biased by data noise. However, the correlation of observed gravity

and topography is biased by the presence of data noise. If  $I$  is uncorrelated with the true gravity signal  $g_{true}$ , it follows that the observed correlation is biased downward by a degree-dependent factor:

$$\gamma_{obs} = \frac{\langle g_{obs} h \rangle}{\sqrt{\langle g_{obs}^2 \rangle \langle h^2 \rangle}} = \gamma_{true} \left( 1 + \frac{\langle I^2 \rangle}{\langle g_{true}^2 \rangle} \right)^{-0.5} \quad (2)$$

where brackets indicate wavelength-dependent expectations of the enclosed quantities. The calculated admittance spectrum at high degrees is similarly biased downward from the Kaula filtering used to produce the gravity field solution, so loading scenarios that fail to fit either the admittance or the correlation at high harmonic degrees should not necessarily be disregarded. Synthetic models of admittance in the presence of random data noise (Fig. 1) are consistent with the biasing term in equation 2.

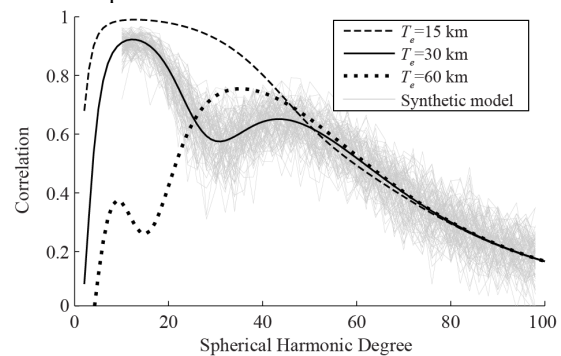


**Figure 1.** Theoretical gravity-topography correlation spectra plotted over 100 synthetic models of gravity-topography correlation for  $T_e=30$  and  $F=0.5$ , with a noisy gravity dataset of degree strength  $l=50$ .

We define a loading parameter  $F$  such that  $F=0$  indicates top loading and  $F=1$  indicates bottom loading, and we assume that top and bottom loads are uncorrelated. Observed gravity-topography admittance and correlation spectra are plotted in Fig. 2. Solid colored lines in Fig. 2 represent noisy gravity with a degree strength of  $l=50$ , and dashed colored lines represent noiseless gravity.

**RMS misfit:** In order to determine best-fit parameter values for Mercury's lithosphere, we calculated a misfit function as a sum of root mean squared (RMS) values for admittance and correlation misfit, where

correlation misfit is scaled such that the minimum correlation misfit equals that of admittance misfit. Normalized misfits between the observed geophysical spectra and theoretical spectra are plotted in Fig. 3. When we reject solutions with misfits more than 25% larger than the minimum misfit, acceptable values of the loading parameter  $F$  fall in the range 0.2–0.6. For  $F=0.5$  (indicating equal top loading and bottom loading), the best-fit elastic thickness is  $T_e=31\pm 9$  km.

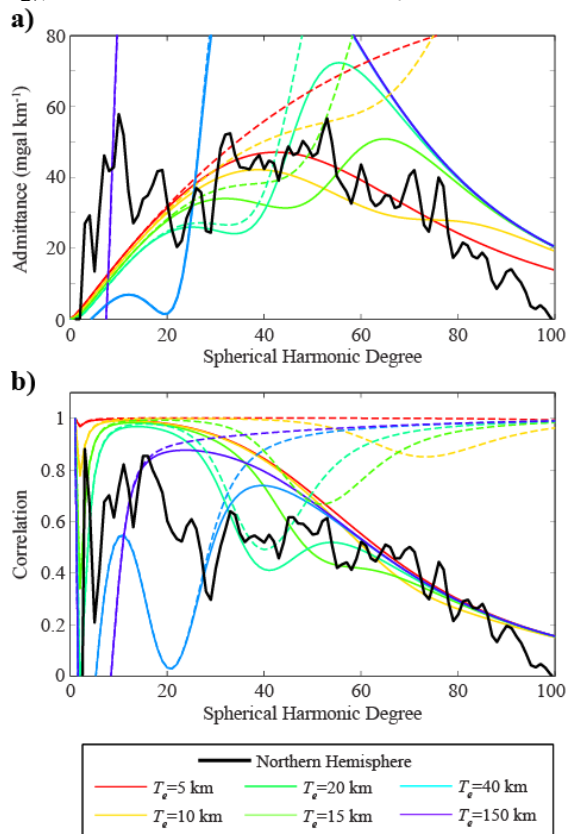


**Figure 2.** (a) Gravity-topography admittance and (b) correlation spectra. Theoretical spectra with noise (colored solid lines) and without noise (colored dashed lines) are plotted over the localized observed spectra.

Our estimate of  $T_e$  is mostly sensitive to gravity and topography at the high latitudes. The present lithosphere thickness is 25-50% greater at the poles than at the equatorial regions due to uneven insolation [7]. Similarly, our geophysical estimate of  $T_e$  is likely higher than the global mean value if Mercury’s rotation pole has not changed significantly over the past ~4 Gyr. The effective elastic lithosphere may be somewhat thinner than the actual mechanical lithosphere if flexural deformation had high curvature [8].

Several measurements of  $T_e$  [see 9,10] are plotted in Fig. 4 over models of crust and lithosphere evolution [10,11]. Our geophysical estimate of  $T_e$  is consis-

tent with an estimate from the depth extent of faulting [9] but is smaller than an estimate from degree-2 gravity and topography [10]. This difference suggests that the lithosphere thickened considerably over the planet’s history. Our estimate of  $T_e$  may have been greater than the contemporaneous crustal thickness (see Fig. 4), which would indicate the presence of a two-layered rheology with the uppermost mantle contributing to the total lithospheric strength.

**References:** [1] Watts A.B. (2001) *Isostasy and Flexure of the Lithosphere*, Cambridge. [2] Turcotte D.L. et al. (1981) *JGR*, 86, 3951–3959. [3] Beuthe M. (2008) *GJI*, 172, 817–841. [4] Audet P. (2014) *PEPI*, 226, 48–82. [5] Genova A. et al. (2015) *EGU*, 5654. [6] Zuber M.T. et al. (2012) *Science*, 335, 217–220. [7] Williams J.-P. et al. (2011) *JGR*, 116, E01008. [8] McNutt M.K. (1984) *JGR*, 89, 11180–11194. [9] Nimmo F. and Watters T.R. (2004) *GRL*, 31, L03701. [10] Tosi N. et al. (2015) *GRL*, 42, 7327–7335. [11] Hauck S.A., II, et al. (2015) *AGU*, P53A-2105.

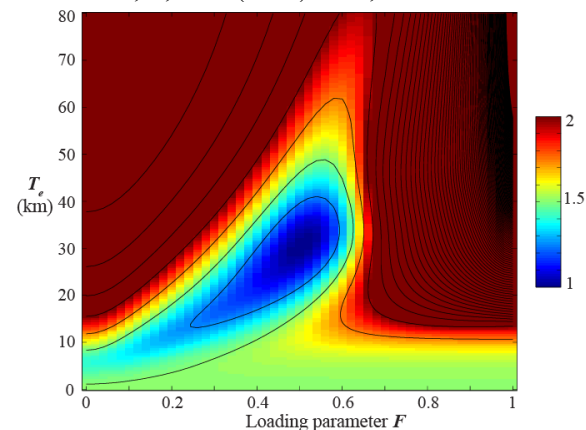


**Figure 3.** Misfit between observed and theoretical spectra versus  $T_e$  and  $F$ , normalized by the lowest misfit.

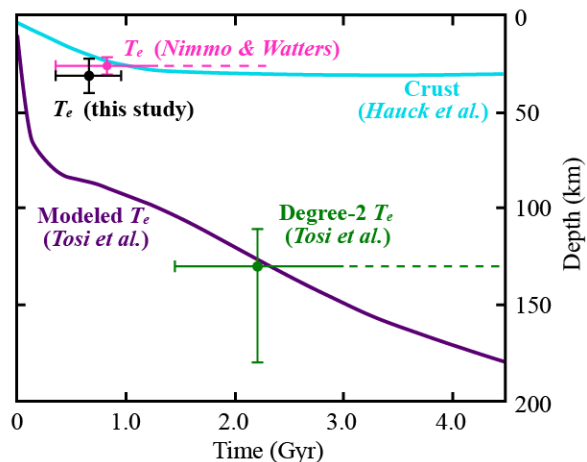


**Figure 4.** Measurements of  $T_e$  compared with models of crust and lithosphere evolution [10,11].